Soft Matter

Dynamic Article Links

Cite this: *Soft Matter*, 2011, **7**, 1747

www.rsc.org/softmatter

PAPER

Specific adhesion between DNA-functionalized "Janus" vesicles: size-limited clusters

Paul A. Beales,† Jin Nam and T. Kyle Vanderlick*

Received 24th September 2010, Accepted 22nd November 2010
DOI: 10.1039/c0sm01055c

Asymmetric building blocks afford assembly of more complex, sophisticated materials than their homogeneous counterparts. Phase separation of mixed membranes produces asymmetric surface textures in lipid vesicles. Membranes that demix into coexisting liquid phases ripen such that the vesicle domain morphology exhibits a Janus-like texture. DNA is commonly used in material science as a molecular glue. Hydrophobically modified DNA strands anchor to the membranes of vesicles such that the DNA is free to bind its complement. When DNA amphiphiles are anchored to phase separated vesicles, they thermodynamically partition between coexisting domains. This results in asymmetric surface distributions of adhesive functionalities. We enhance the partitioning of cholesteryl-anchored DNA into liquid ordered (L_o) domains of Janus-like vesicles by incorporating highly unsaturated lipids into membrane mixtures. We find that cardiolipin (CL) drives the strongest enrichment of DNA into L_o domains with apparent surface concentrations at least an order of magnitude greater than in coexisting liquid disordered domains. We also examine the partitioning of DNA with a lipid-like anchor in Janus-textured vesicles; the inclusion of CL also drives a very strong enhancement into L_o domains. The culmination of this work is the study of superstructures that form when populations of these Janus vesicles, functionalized by complementary DNA strands, are mixed. Unlike their homogeneous counterparts, which can form uncontrollably large clusters, size-limited multicompartmental architectures are observed. The DNA-rich L_o domains saturate in adhesion plaques of the clusters. This predominantly leaves DNA-depleted L_α phase accessible on the exterior surface of these structures, which does not favor binding of further vesicles.

Introduction

Much of the recent focus in the assembly of hard colloidal particles has been related to the fabrication of patchy building blocks and the structures that can be formed when they interact with one another.[1–4] These anisotropic particles have a heterogeneous surface chemistry such that their interactions are not just dependent upon the inter-particle separations but also have a strong dependence upon the particles' relative orientations. This added degree of complexity allows greater control and sophistication in the array of possible supra-particular materials that can be assembled from these principal constituents. A significant proportion of work in this area has been concerned with Janus particles,[5] a sub-class of anisotropic particles with two opposing faces with disparate surface chemistry.

Similar, Janus-like morphologies can be formed in soft, self-assembled architectures composed of amphiphilic molecules, *e.g.* lipids. In vesicles composed of lipid mixtures, which preferentially demix into coexisting liquid-like phases, the membrane domains coalesce over time (to minimize interfacial line tension between phases) until the vesicles are composed of two opposing domains of differing chemical composition.[6–8] Thermodynamic partitioning of functional amphiphiles, *e.g.* specific adhesion molecules, between the coexisting domains is one possible route to controllably creating directional interactions between these liposomes. DNA, in particular, is a class of molecules that has gained significant popularity for use as a molecular glue in the assembly of nanoscale and microscale materials.[9–14] This is mainly due to its highly specific, sequence dependent binding that allows many different DNA sequences to be utilized in encoding the association of complex materials.

The strength of attraction between lipid vesicles can be controlled through incorporation of DNA-amphiphiles within the vesicle membrane.[15–20] Single-stranded DNA with a hydrophobic modification on one of its ends inserts into the membrane of pre-formed lipid vesicles such that the nucleic acid sequence extends from the bilayer and is free to bind its complement.[17,21–24] Commonly used hydrophobic anchors are either a cholesterol-like[17,18,21,25–27] or a lipid-like[16,28] moiety. Populations of vesicles

Department of Chemical Engineering, Yale University, New Haven, CT, 06511, USA. E-mail: kyle.vanderlick@yale.edu; Fax: +1 203 432 0358; Tel: +1 203 432 4220

† Present address: Centre for Molecular Nanoscience, School of Chemistry, University of Leeds, Leeds LS2 9JT, UK.

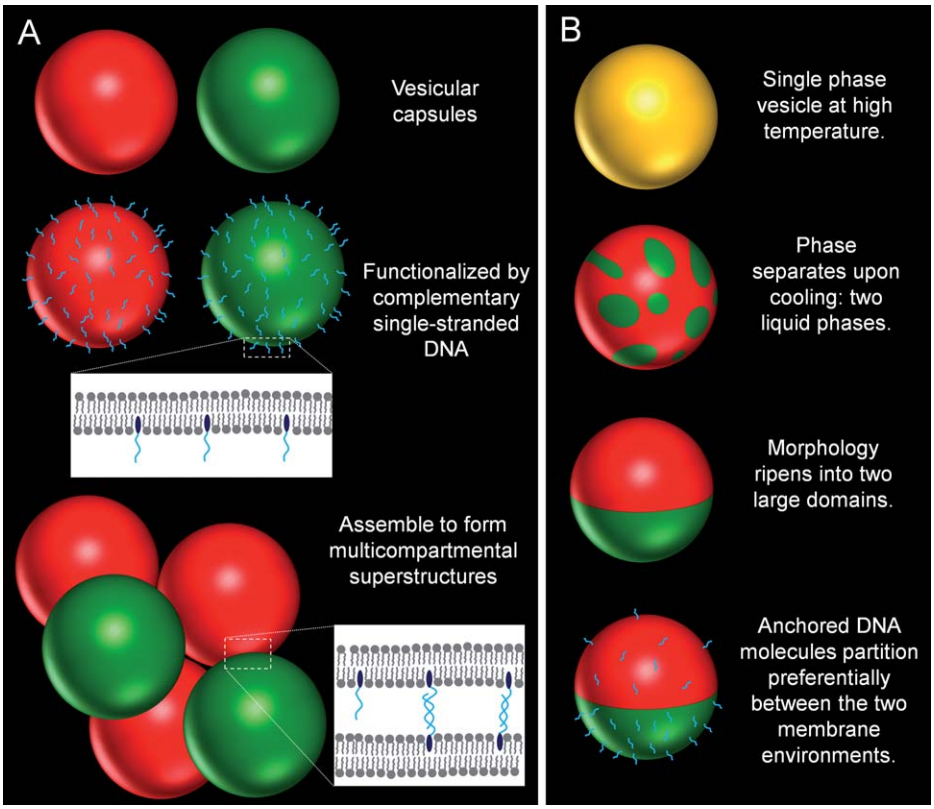

Fig. 1 (A) Functionalization of liposomal capsules with complementary, hydrophobically modified DNA sequences allows the formation of multicompartmental liposomal clusters through specific hybridization of the membrane-anchored DNA strands. (B) Liposomes can be formed, composed of lipid mixtures that are well mixed at high temperatures, but phase separate into coexisting fluid phases at room temperature. The domain morphology ripens into two large domains, one of each phase. When these liposomes are functionalized by hydrophobically modified DNA molecules, the DNA functionalities partition between the coexisting phases resulting in domains of differing DNA surface density.

functionalized by complementary DNA sequences, when mixed, adhere to form multicompartmental clusters[17,18] (Fig. 1A). The soft membranes can deform due to the strength of inter-vesicle adhesion to create extended adhesion plaques with multiple DNA bonds between conjoined vesicles.[17] This aspect differs from the DNA-mediated assembly of hard particles, which are not known to deform upon association.[29–35]

DNA-amphiphiles can also be anchored to phase separated vesicles, *e.g.* Janus-like vesicles composed of two fluid phases, where they preferentially partition between coexisting domains[24,36–38] (Fig. 1B). Their phase partitioning behavior is dependent upon the structure of their hydrophobic anchor and the composition of the membrane. In this paper we will modify the lipid composition of Janus-like vesicles to enhance the segregation of DNA-amphiphiles in these systems. For the first time, we investigate the morphologies of the structures that form within mixed populations of DNA-functionalized Janus vesicles bearing complementary sequences.

Experimental

Materials

Cholesterol-modified DNAs (chol–DNAs) were purchased from Eurogentec North America: sequences cholesteryl-TEG-5′-ACA GAC TAC C-3′ (chol–DNA10-1), cholesteryl-TEG-5′-TTT CCG GGC GGC GCG GGG CGG GGA CAG ACT ACC-3′ (chol–DNA30-1), cholesteryl-TEG-5′-TTT CCG GGC GGC GCG GGG CGG GGG GTA GTC TGT-3′ (chol–DNA30-2) and cholesteryl-TEG-3′-TTT GGC CCG CGC CCC GCC CC-5′ (chol–DNA20). Double-anchored chol–DNA hybrid pairs were prepared by mixing stoichiometric amounts of chol–DNA20 with chol–DNA30-1 or chol–DNA30-2 to create bivalent cholesterol chol–DNA30-1/chol–DNA20 or chol–DNA30-2/chol–DNA20 molecules.[21] Alexa Fluor 647 (A647) labeled DNA was purchased from IDT (A647-5′-GGT AGT CTG T-3′; A647–DNA).

N-(7-Nitrobenz-2-oxa-1,3-diazol-4-yl)-1,2-dihexadecanoyl-*sn-glycero*-3-phosphoethanolamine, triethylammonium salt (NBD-DPPE) was obtained from Invitrogen—Molecular Probes. All other lipids were ordered from Avanti Polar Lipids: 1,2-dipalmitoyl-*sn-glycero*-3-phosphocholine (DPPC), 1,2-dioleoyl-*sn-glycero*-3-phosphocholine (DOPC), 1,2-dilinoleoyl-*sn-glycero*-3-phosphocholine (DC18:2PC), 1,2-dilinolenoyl-*sn-glycero*-3-phosphocholine (DC18:3PC), 1,2-diarachidonoyl-*sn-glycero*-3-phosphocholine (DC20 : 4PC), 1,2-didocosahexaenoyl-*sn-glycero*-3-phosphocholine (DC22 : 6PC), bovine heart cardiolipin (CL), cholesterol (chol) and 1,2-dioleoyl-*sn-glycero*-3-phosphoethanolamine-*N*-(lissamine rhodamine B sulfonyl) (ammonium salt) (Rh-DOPE).

Dialkyl lipid–DNA (lipid–DNA) was synthesized based upon the protocol of Chan *et al.*[16] 1,2-*O*-Dioctadecyl-*rac*-glycerol was

purchased from Chem-Impex and 2-cyanoethyl *N*,*N*-diisopropylchlorophosphoramidite was purchased from Sigma. 0.4 g of 1,2-*O*-dioctadecyl-*rac*-glycerol (0.66 mmol) and 0.3 mL diisopropylethylamine (17 mmol) were dissolved in 20 mL anhydrous dichloromethane at 0 °C under an argon atmosphere. 0.3 g 2-cyanoethyl *N*,*N* diisopropylchlorophosphoramidite (1.5 mmol) was added dropwise to the reaction, which was stirred at 0 °C for 30 minutes then at room temperature for 6 hours. The crude product solution was washed with a 0.5 M solution of sodium bicarbonate. The solvent was evaporated before redissolving the lipid–phosphoramidite to 0.1 M in dichloromethane. The dioctadecyl lipid phosphoramidite was added as the final base on a DNA synthesizer. We use a lipid–DNA conjugate with the base sequence: dioctadecyl lipid-5′-TTT ACA GAC TAC C-3′ (lipid–DNA1). Successful lipid–DNA conjugation was checked by mass spectrometry.

Sample preparation

Giant Unilamellar Vesicles (GUVs) were formed by the electroformation method. Briefly, 20–70 μL of 1.0 mM lipid mixtures in chloroform at the desired molar ratio was placed dropwise onto the platinum wires of a home-built electroformation chamber. The solvent was removed overnight, under vacuum. Electroformation was conducted in an oven at temperatures above 50 °C, comfortably higher than the highest melting transition of any lipid in the mixture (DPPC, 41 °C). A pre-heated 300 mM sucrose solution was added carefully to the chamber so as to minimize air bubbles; a function generator was used to apply an AC field across the platinum wires (3 V or 1 V if the mixture contained anionic lipids; 10 Hz for 30 min, 3 Hz for 15 min, 1 Hz for 7 min, 0.5 Hz for 7 min). The vesicles were then removed from the chamber and allowed to slowly cool to room temperature.

A minimum of one hour was allowed for phase separation and ripening of domain morphology in the GUV samples before mixing the hydrophobically modified DNA with the GUVs at the desired lipid : DNA ratios. Samples were then placed on a nutator to mix for several hours to allow the DNA functionalities to anchor to the pre-formed vesicles. For experiments to investigate the partitioning of the anchored DNA between phases, a stoichiometric amount of A647–DNA was added to the GUVs along with an iso-osmolar sodium chloride solution buffered with 10 mM HEPES to pH 7.4 such that the final sodium ion concentration in the samples was 100 mM. The samples were then returned to the nutator for at least one further hour before imaging in order to allow the fluorescent DNA to bind to its membrane-anchored complement. For experiments to investigate the self-assembly behavior of complementary Janus vesicles, equal amounts of GUVs functionalized with complementary DNA sequences were mixed and the sodium ion concentration was adjusted as desired with the iso-osmolar HEPES-buffered sodium chloride solution (pH 7.4). Samples were then returned to the nutator to mix overnight before they were imaged.

Laser-scanning confocal microscopy

Imaging was conducted on a Leica TCS SP5 confocal microscope. Samples were placed into glass bottom culture dishes (MatTek Corporation, part no. P35G-1.5-20-C) for observation. These dishes had been treated with a 10% bovine serum albumin solution in order to prevent GUVs adhering to the cover glass.

Results and discussion

We first investigate the prospect of enhancing the partitioning of cholesterol-modified DNAs (chol–DNAs) between coexisting liquid phases of GUVs. We also investigate the partitioning of a dialkyl lipid-modified DNA (lipid–DNA) in these Janus-textured vesicles. Once we have identified the lipid mixture that provides the strongest partitioning of membrane-anchored DNA between the liquid domains, we functionalize two populations of Janus vesicles with complementary DNA sequences. The culmination of this work is the investigation of cluster morphologies between adhering Janus vesicles. We mix these GUVs at a range of salt concentrations and observe the architectures of the multicompartmental structures that assemble.

It is already known that the partitioning of cholesterol-modified DNA in Janus-textured GUVs is dependent upon the lipid composition and anchor geometry.[38] We have previously reported a slight enhancement of single cholesterol modified DNA in the liquid-ordered (L_o) phase of phase separated GUVs composed of DOPC/DPPC/chol. However, we also found that DNA functionalities anchored to membranes of the same composition through two cholesterol anchors showed a stronger partitioning into the L_o phase, with concentrations up to approximately a factor of two greater than the liquid-disordered (L_α) phase. We interpreted this observation as an entropic unfavorability for the rigid cholesterol backbone of the anchor to sit next to kinked, unsaturated lipid tails driving the increased enhancement of double cholesterol anchored lipids into the L_o phase. Here, we incorporate more highly unsaturated lipids into phase-separating lipid mixtures with the hope of driving even stronger partitioning of cholesterol-modified DNAs into the L_o domains.

GUVs containing highly unsaturated lipids still phase separate into coexisting liquid phases. We made GUVs containing 3 : 3 : 6 : 4 DOPC : (highly unsaturated lipid) : DPPC : chol, where the highly unsaturated lipids tested were DC18:2PC, DC18:3PC,DC20:4PC and DC22:6PC. Upon cooling, their membranes phase separate into two liquid phases: domain morphologies ripen over time by coalescence until the membrane consists of two large regions, one of each phase. We also make phase separated vesicles containing 10 mol% CL, replacing 10 mol% of DOPC in 3 : 3 : 2 DOPC : DPPC : chol lipid mixtures.

The apparent partitioning of DNA amphiphiles between coexisting phases can be visualized by confocal fluorescence microscopy (Fig. 2). Phase separated vesicles are functionalized with cholesterol-modified DNA (either chol–DNA10-1 or chol–DNA30-1/chol–DNA20) or a lipid-modified DNA that was first reported by Chan *et al.*[16] DNA amphiphiles were added to vesicles at surface concentrations of less than 10^{-2} DNA/lipid. Upon adding a stoichiometric amount of fluorescent, complementary DNA (A647–DNA), in the presence of sufficient salt ions (100 mM NaCl, which results in a duplex melting temperature under these conditions of at least 10 °C above room temperature for the unmodified sequences in free solution[39]), these reporter molecules hybridize with the membrane-bound

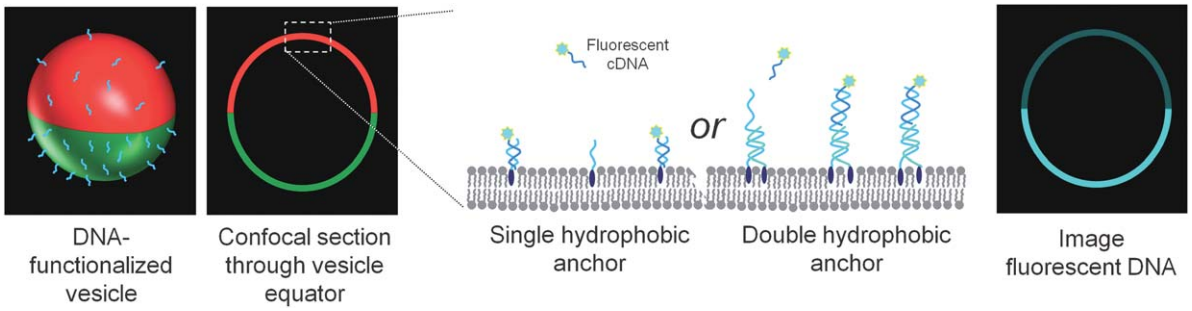

Fig. 2 DNA-functionalized, phase separated vesicles are imaged by confocal fluorescence microscopy. Confocal imaging through the equator of the vesicles yields thin optical sections that appear as membrane "rings" in the resultant image. The apparent partitioning of DNA functionalities between coexisting phases can be observed through the fluorescence intensity of a DNA complement bound to each phase.

DNA. The salt ions are required to screen the electrostatic repulsion between the sugar–phosphate backbones of the DNA strands, which competes against the hydrogen-bonding and π-stacking interactions that favor duplex formation.[40–42] Confocal microscopy provides thin optical sections through the vesicle such that the membrane appears as a fluorescent ring in the image. The apparent partitioning of the DNA amphiphiles between phases can be observed by analysis of the fluorescence intensity of the A647 dye in each domain.

Highly unsaturated lipids enhance partitioning of DNA into the L_o phase

We find that inclusion of highly unsaturated lipids in the phase separating membrane compositions enhances the partitioning of chol–DNAs into the L_o phase. Example confocal image sections and intensity line profiles through GUVs of these compositions are shown in Fig. 3, where the fluorescent lipid analogue Rh-DOPE (red, 0.5 mol%) labels the L_α phase. Analysis of the intensity of A647–DNA (blue) in each phase reveals an apparent partitioning of chol–DNAs into the L_o phase by up to a factor of approximately three, dependent upon the anchoring geometry and membrane composition. The apparent partitioning that we observe when incorporating more highly unsaturated lipids into the membrane mixtures shows a stronger preference for the L_o phase than we have previously observed for simpler DOPC/DPPC/chol GUVs.[38] We also find the double-chol anchored DNAs partition more strongly into the L_o phase than single-chol anchored DNAs for a given membrane composition, similar to what we previously reported for the ternary mixtures.[38]

Of all the highly unsaturated lipids we evaluated, we find that inclusion of CL in the membrane mixtures drives the strongest partitioning of chol–DNAs into the L_o phase. CL has an unusual lipid structure as it consists of four symmetric acyl tails (as opposed to two); each of these tails is 18 carbons long and contains two unsaturated bonds. GUVs were prepared with 10 mol% CL replacing 10 mol% DOPC in 3 : 3 : 2 DOPC : DPPC : chol mixtures. These vesicles phase separate into coexisting liquid phases with CL strongly segregated in the L_α phase.[43] Fig. 4 shows the partitioning of double-chol DNA within these CL-containing GUVs. The A647–DNA indicates a very strong sequestering of the chol–DNA in the L_o phase: the apparent partitioning from intensity line profiles indicates that the concentration of chol–DNA in the L_o phase is at least an order greater than that in the L_α phase, with the fluorescence signal from the A647–DNA emanating from L_α domains being hardly detectable. The 3D reconstruction of a GUV hemisphere from individual confocal sections, shown in Fig. 4c, clearly demonstrates the Janus-like morphology of these vesicles.

CL also strongly influences the membrane localization of a lipid anchored DNA. We analyze the phase partitioning behavior of a lipid-modified DNA[16,28] with two symmetric, saturated 18 carbon alkyl tails. Phase separated GUVs were functionalized with lipid–DNA1 and A647–DNA was added as a marker to elucidate its partitioning behavior. Whilst the structure of this hydrophobic anchor is very different to that of the chol moieties that we have previously studied, the partitioning of these molecules is also strongly dependent on membrane composition, as shown in Fig. 5. In GUVs composed of 3 : 3 : 2 DOPC : DPPC : chol, the lipid–DNA shows an apparent partitioning approximately two to three times higher in the L_o phase than in L_α domains. However, when 10 mol% CL is incorporated into the phase separating mixture, this also drives the lipid–DNA strongly into the L_o domains. Similarly to the chol–DNAs with a divalent cholesteryl anchor, the fluorescence intensity from the A647–DNA in the L_α phase is hardly detectable with an apparent partitioning of at least an order of magnitude into the L_o domains.

The potency of CL at driving these DNA functionalities into the L_o phase could be a result of lateral packing stresses created in the L_α domains. CL is well known to prefer regions of membrane with negative curvatures (that bend towards the aqueous phase) and in some circumstances forms inverted hexagonal phases.[44,45] Inclusion of negative curvature lipids, *e.g.* CL, in lipid bilayers increases lateral packing stresses in the hydrophobic regions of the membrane.[46] Such packing stresses may act to increase the free energy cost of insertion of chol–DNAs and lipid–DNAs into the L_α phase and thereby strongly enhance their partitioning into L_o domains.

Assembly of "Janus" vesicles into size-limited clusters

Now that we have created Janus vesicles with a very significant enhancement of DNA functionalities in the L_o domains, we will investigate the assembly of these soft, anisotropic capsules. Two populations of Janus vesicles decorated with complementary DNA sequences are mixed such that inter-vesicle adhesion can occur through DNA hybridization reactions. Whilst we have

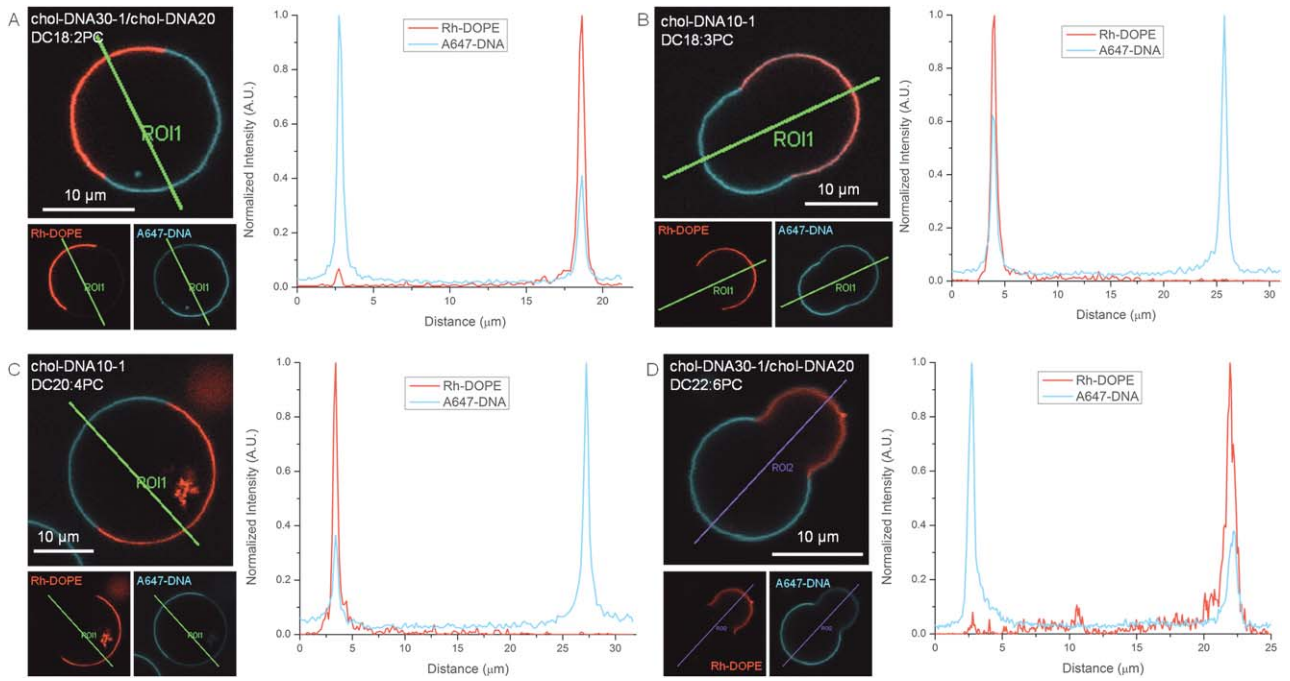

Fig. 3 Example confocal sections and intensity line profiles for the partitioning of chol–DNAs in phase separated GUVs containing a highly unsaturated lipid. Lipid probe Rh-DOPE (red) labels the L_α phase; A647–DNA (blue) elucidates the location of chol–DNAs anchored to the vesicles. (A) 3 : 3 : 6 : 4 DOPC : DC18:2PC : DPPC : chol GUV functionalized with chol–DNA30-1/chol–DNA20; (B) 3 : 3 : 6 : 4 DOPC : DC18:3PC : DPPC : -chol GUV functionalized with chol–DNA10-1; (C) 3 : 3 : 6 : 4 DOPC : DC20:4PC : DPPC : chol GUV functionalized with chol–DNA10-1; (D) 3 : 3 : 6 : 4 DOPC : DC22:6PC : DPPC : chol GUV functionalized with chol–DNA30-1/chol–DNA20. The green (A–C) and magenta (D) line profiles in the images represent the locations of the intensity line profiles displayed in the adjacent graphs.

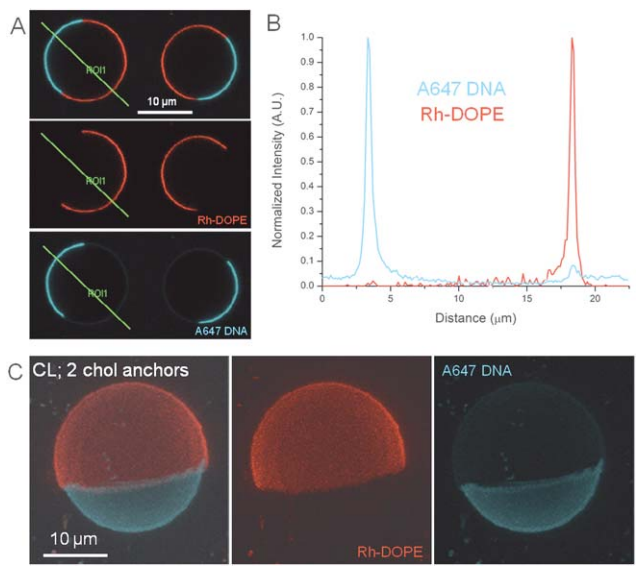

Fig. 4 (A) Images showing the partitioning of chol–DNA30-1/chol–DNA20 between coexisting liquid phases in 10 mol% CL phase separated GUVs. (B) Example intensity line profile through the two phases (the line section being depicted by the green line in part A). (C) 3D reconstruction from individual confocal image sections showing the morphology of a hemisphere of a 10 mol% CL phase separated GUV functionalized by chol–DNA30-1/chol–DNA20. Rh-DOPE (red) marks the location of the L_α phase; A647–DNA (blue) shows the partitioning of membrane-anchored DNA between coexisting phases.

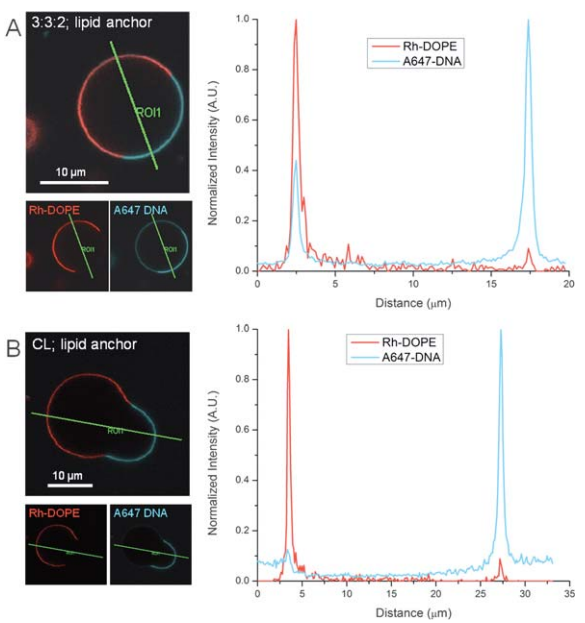

Fig. 5 (A) Partitioning of lipid–DNA in 3 : 3 : 2 DOPC : DPPC : chol. The graph shows an example intensity line profile (marked in green in the images) through both phases. (B) Partitioning of lipid–DNA in 10 mol% CL phase separated GUVs. The position of the example intensity line profile through the coexisting phases is also marked on the image in green.

previously seen that GUVs with homogeneous surface distributions of DNA can bind into uncontrollably large agglomerates,[17] here we will show that the Janus-texturing of vesicles provides a size-limiting mechanism to the cluster architectures.

We assemble multicompartmental superstructures with complementary populations of DNA-functionalized CL-containing, phase separated GUVs (CLPS-GUVs) that exhibit a Janus domain morphology. We have already demonstrated that the surface distribution of DNA functionalities in these vesicles is highly asymmetric. One population of CLPS-GUVs was functionalized by either chol–DNA30-1/chol–DNA20 or lipid–DNA1. A second set of CLPS-GUVs was functionalized by chol–DNA30-2/chol–DNA20. Bulk surface concentrations of DNA were approximately 3×10^{-3} DNA/lipid for each vesicle population. Both sets of vesicles were labeled with 0.5 mol% Rh-DOPE (red), which partitions into the L_α phase, and 0.5 mol% NBD-DPPE (green), which partitions into the L_o domains. These two vesicle populations, bearing complementary DNA functionalities, were mixed in solutions at various ionic strengths.

Populations of CLPS-GUVs functionalized with complementary DNA strands adhere through their L_o domains. Finite clusters of adhering CLPS-GUVs are shown in Fig. 6. At very low ionic strengths (below ~10–18 mM NaCl), the CLPS-GUVs do not adhere and remain as individual, isolated vesicles in solution (under these conditions, the melting temperatures of these DNA strands, in free solution, are approximately in the range of 10–16 °C;[39] this is also consistent with the phase diagram for DNA-mediated adhesion between homogeneous GUVs that we have previously reported using the same 10 base recognition sequences[17]). As the ionic strength is increased, DNA hybridization becomes more favorable due to electrostatic screening of the repulsion between the charged backbones of the DNA strands. We begin to observe adhesion between CLPS-GUVs: this adhesion is exclusively through the L_o domains of the vesicles, where the DNA functionalities are strongly segregated (Fig. 6A–L).

The number of vesicles and structure of a cluster are likely to be, at least in part, a consequence of size differences between the adhering vesicles. For example, smaller vesicles will not take up

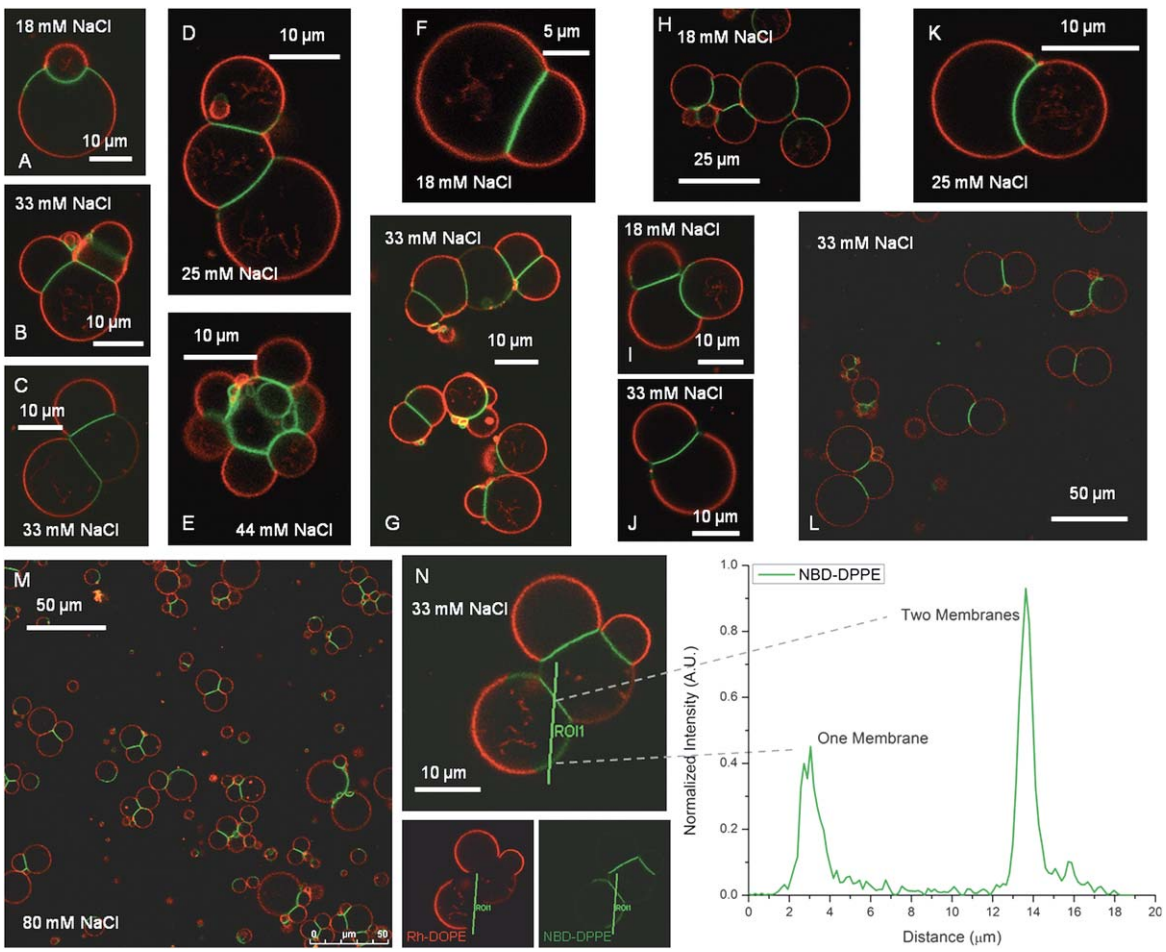

Fig. 6 Size-limited clusters of DNA-functionalized Janus vesicles. Sodium chloride concentrations are noted on each image. Vesicles are labeled with lipid probes Rh-DOPE (red), which partitions into L_α domains, and NBD-DPPE (green), which labels the L_o phase. Images C, E, J, L, M and N have one vesicle population functionalized by lipid–DNA1 and a second population functionalized by chol–DNA30-2/chol–DNA20; in all other images the first vesicle set is functionalized with chol–DNA30-1/chol–DNA20 instead of lipid–DNA1. Part N shows the individual Rh-DOPE and NBD-DPPE channels as well as the composite image. An intensity line profile is shown through a section of the L_o phase in the adhesion plaque and an unbound region of the L_o domain: this clearly demonstrates that two membranes are present in the adhesion plaque.

the entire L_o domain of a much larger GUV in the adhesion plaque, leaving excess L_o domain area accessible for further vesicle(s) to bind. In some cases, a few CLPS-GUVs had not fully ripened into a Janus-like morphology of one domain of each phase. When more than one L_o domain is present on a GUV in a cluster, this can lead to the formation of more extended structures containing a larger number of vesicles, *e.g.* Fig. 6B, D, G, and H.

Adhesion between complementary Janus CLPS-GUVs results in size-limited clusters of vesicles. At high ionic strengths, where large-scale aggregates have been reported for homogeneous, single phase GUVs,[17] small clusters of vesicles are still observed (Fig. 6M). The DNA-rich L_o domains of the vesicles in these clusters are taken up in the adhesion plaques. Due to the soft, deformable nature of lipid membranes, the adhesive energy between vesicles causes the CLPS-GUV membranes to flatten, forming large, extended contact zones between bound vesicles. The result of this is that the L_o domains of the vesicles become buried inside these composite structures, leaving almost exclusively L_α phase membrane on the accessible surface of the clusters. The L_α phase is strongly depleted in DNA functionalities and hence further association with other vesicles or vesicle agglomerates becomes highly unfavorable, limiting the size of the clusters. Clusters were observed ranging in size from two vesicles up to, in extreme cases, approximately 10 vesicles. Very few assembly defects are observed in these samples at high ionic strength, where L_α domains form one or both membrane of an adhesion plaque.

The membranes of CLPS-GUVs do not fuse in the adhesion plaques between vesicles. Fig. 6N shows an intensity line profile for NBD-DPPE through the adhesion plaque between two vesicles and a portion of the L_o domain of a vesicle that is not taken up by adhesion to another vesicle. The fluorescent intensity in the adhering area of membrane is approximately double that of the unbound membrane. This indicates that two distinct membranes exist in the adhesion plaque, such that the membranes have not fused. This is consistent with the reversibility of binding between DNA-functionalized vesicles, as has previously been reported.[17,18]

The size-limiting effect of the Janus vesicle clustering can be understood by considering a simplified model for adhesion between individually weak specific bonds.[38] Fig. 7 depicts a simplified model phase diagram for adhesion between particles *via* many weak, specific bonds or receptors: one axis represents the strength of the individual bonds and the other axis represents the surface density of bonds. At lower bond strengths, a higher surface concentration of adhesion molecules is required for binding to occur: a large number of bonds need to act cooperatively for long term adhesion to occur. We can consider that the strength of individual DNA bonds is controlled through the ionic strength of the aqueous media. A similar dependency for adhesion between DNA-functionalized, single phase vesicles with varying DNA loading on the vesicles and ionic strength of the surrounding media has been demonstrated.[17]

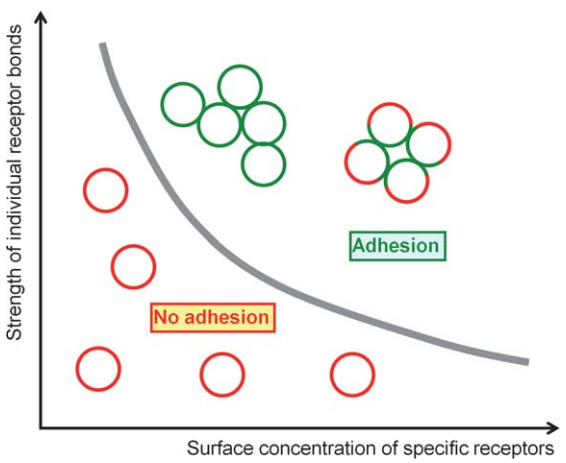

Fig. 7 A simple model of a phase diagram for adhesion between particles *via* weak specific bonds.

For the case of adhesion between CLPS-GUVs, whilst the strength of each potential DNA bond is the same for molecules anchored to either phase (at constant ionic strength), the surface concentration of DNA "receptors" is strongly dependent on the phase of the domain. Therefore, the DNA in the L_o phase can be in an environment that favors adhesion, whereas the DNAs in the L_α phase of the same vesicle can be in a state that disfavors binding. This unfavorability for binding between DNA-depleted domains is likely enhanced by the lower probability of DNA bonds forming during a collision due to their low surface density.[15] Electrostatic repulsion between anionic, CL-containing L_α regions of membrane will further diminish the favorability of DNA binding between the L_α domains.[18] These latter two considerations presumably augment the low proportion of assembly errors (or defects) observed at higher ionic strengths, where DNA-depleted L_α domains contribute to an adhesion plaque.

Our observations of binding interactions between these Janus vesicles are consistent with a phase diagram for homogeneous, single phase GUVs, functionalized with the same 10 base recognition sequences that we previously reported.[17] We make the simplifying assumptions that our CLPS-GUVs consist of 50% L_α phase and 50% L_o phase, by surface area, and take the partitioning coefficient of anchored DNA functionalities between phases to be 10. This would mean that GUVs with an average total surface concentration of 3×10^{-3} DNA/lipid would have 5.5×10^{-4} DNA/lipid in the L_α phase and 5.5×10^{-3} DNA/lipid in the L_o phase. Over this range of DNA surface concentrations, no binding was observed between homogeneous GUVs at ionic strengths below 20 mM.[17] Above this salt concentration, small clusters and unitary GUVs were observed for homogeneous GUVs with a DNA surface coverage consistent with that of the L_o phase (5.5×10^{-3} DNA/lipid), up to approximately 45 mM [Na^+]. Above 45 mM [Na^+], GUVs at this higher surface coverage form extremely large clusters of uncontrollable size. However, at lower surface concentrations consistent with the L_α phase (5.5×10^{-4} DNA/lipid), no GUV adhesion between homogeneous GUVs is observed over the range of ionic strengths investigated. This comparison to previous findings for single phase GUVs supports our interpretation of the size-limiting mechanism for clustering of our Janus vesicles and the qualitative model presented in Fig. 7.

Summary and outlook

DNA-functionalized giant lipid vesicles with a "Janus"-like domain morphology can be assembled into size-limited,

multicompartmental architectures. We have demonstrated that the partitioning of DNA functionalities between lipid phases is strongly dependent on the lipid composition of each phase. CL-containing, phase separated vesicles drive strong partitioning of both bivalent cholesterol and dialkyl lipid anchors into the L_o domains. When two populations of these phase separated vesicles, functionalized with complementary DNA sequences, are mixed in the presence of sufficient salt ions, these vesicles assemble into size-limited clusters. The DNA-rich L_o domains are taken up in the extended adhesion plaques inside the clusters leaving the DNA-depleted L_α domains, which do not favor further binding, exposed on the accessible outer surface of these structures.

Size-limited configurations similar to those demonstrated here may find applications in drug delivery. Multicompartmental encapsulation strategies could be advantageous for the simultaneous *in vivo* delivery of multiple therapeutics, diagnostics and imaging agents.[47,48] These active components would be kept in physical isolation during transport in order to avoid adverse interactions with one another or to maintain each agent within different, favorable environments. For many therapeutic delivery strategies, it is likely that multicompartmental clusters would preferably be created on sub-micron lengthscales, *i.e.* scaled down in size from the structures we demonstrate here.

Similar modular architectures may also find use in bottom-up strategies for the nascent field of synthetic biology. Synthetic biology is an emerging field which aims to engineer novel biochemical modules to undertake functions not normally found in nature.[49–51] Current strategies usually involve the top-down addition of biochemical modules to host cells, often referred to as chassis. In the future, bottom-up self-assembly may also become a feasible approach, where liposomal chassis act as minimal cells that encapsulate the biochemical machinery of the synthetic modules.[52–54] This approach would minimize biological cross-talk between synthetic modules and the biochemistry of the host. Indeed, multiple liposomal capsules could encapsulate different modules with input and output machinery communicating signals between compartments. This kind of modular network strategy would mimic the multicompartmentalization of natural organs, cells and their organelles.

Acknowledgements

We thank the W. M. Keck Foundation Biotechnology Resource Facility at Yale University for the oligonucleotide synthesis of the lipid–DNA conjugates.

References

1 A. B. Pawar and I. Kretzschmar, *Macromol. Rapid Commun.*, 2010, **31**, 150–168.
2 S. Jiang, Q. Chen, M. Tripathy, E. Luijten, K. S. Schweizer and S. Granick, *Adv. Mater.*, 2010, **22**, 1060–1071.
3 A. Walther and A. H. E. Muller, *Soft Matter*, 2008, **4**, 663–668.
4 F. Wurm and A. F. M. Kilbinger, *Angew. Chem., Int. Ed.*, 2009, **48**, 8412–8421.
5 P. G. de Gennes, *Rev. Mod. Phys.*, 1992, **64**, 645–648.
6 S. L. Veatch and S. L. Keller, *Phys. Rev. Lett.*, 2002, **89**, 268101.
7 S. L. Veatch and S. L. Keller, *Biophys. J.*, 2003, **85**, 3074–3083.
8 S. Semrau and T. Schmidt, *Soft Matter*, 2009, **5**, 3174–3186.
9 T. H. LaBean and H. Y. Li, *Nano Today*, 2007, **2**, 26–35.
10 X. D. Liu, M. Yamada, M. Matsunaga and N. Nishi, in *Functional Materials and Biomaterials*, Springer-Verlag, Berlin, 2007, pp. 149–178.
11 C. M. Niemeyer, *Curr. Opin. Chem. Biol.*, 2000, **4**, 609–618.
12 N. C. Seeman, *Nature*, 2003, **421**, 427–431.
13 J. J. Storhoff and C. A. Mirkin, *Chem. Rev.*, 1999, **99**, 1849–1862.
14 N. Geerts and E. Eiser, *Soft Matter*, 2010, **6**, 4647–4660.
15 Y. H. M. Chan, P. Lenz and S. G. Boxer, *Proc. Natl. Acad. Sci. U. S. A.*, 2007, **104**, 18913–18918.
16 Y.-H. M. Chan, B. van Lengerich and S. G. Boxer, *Biointerphases*, 2008, **3**, FA17–FA21.
17 P. A. Beales and T. K. Vanderlick, *J. Phys. Chem. A*, 2007, **111**, 12372–12380.
18 P. A. Beales and T. K. Vanderlick, *Biophys. J.*, 2009, **96**, 1554–1565.
19 A. Gunnarsson, P. Jonsson, R. Marie, J. O. Tegenfeldt and F. Hook, *Nano Lett.*, 2008, **8**, 183–188.
20 G. Stengel, L. Simonsson, R. A. Campbell and F. Hook, *J. Phys. Chem. B*, 2008, **112**, 8264–8274.
21 I. Pfeiffer and F. Hook, *J. Am. Chem. Soc.*, 2004, **126**, 10224–10225.
22 C. Yoshina-Ishii and S. G. Boxer, *J. Am. Chem. Soc.*, 2003, **125**, 3696–3697.
23 M. Banchelli, F. Betti, D. Berti, G. Caminati, F. B. Bombelli, T. Brown, L. M. Wilhelmsson, B. Norden and P. Baglioni, *J. Phys. Chem. B*, 2008, **112**, 10942–10952.
24 A. Kurz, A. Bunge, A. K. Windeck, M. Rost, W. Flasche, A. Arbuzova, D. Strohbach, S. Mueller, J. Liebscher, D. Huster and A. Herrmann, *Angew. Chem., Int. Ed.*, 2006, **45**, 4440–4444.
25 B. Stadler, D. Falconnet, I. Pfeiffer, F. Hook and J. Voros, *Langmuir*, 2004, **20**, 11348–11354.
26 M. Banchelli, F. Gambinossi, A. Durand, G. Caminati, T. Brown, D. Berti and P. Baglioni, *J. Phys. Chem. B*, 2010, **114**, 7348–7358.
27 F. B. Bombelli, F. Betti, F. Gambinossi, G. Caminati, T. Brown, P. Baglioni and D. Berti, *Soft Matter*, 2009, **5**, 1639–1645.
28 M. Chung, R. D. Lowe, Y. H. M. Chan, P. V. Ganesan and S. G. Boxer, *J. Struct. Biol.*, 2009, **168**, 190–199.
29 C. A. Mirkin, R. L. Letsinger, R. C. Mucic and J. J. Storhoff, *Nature*, 1996, **382**, 607–609.
30 S. Y. Park, A. K. R. Lytton-Jean, B. Lee, S. Weigand, G. C. Schatz and C. A. Mirkin, *Nature*, 2008, **451**, 553–556.
31 D. Nykypanchuk, M. M. Maye, D. van der Lelie and O. Gang, *Nature*, 2008, **451**, 549–552.
32 M. P. Valignat, O. Theodoly, J. C. Crocker, W. B. Russel and P. M. Chaikin, *Proc. Natl. Acad. Sci. U. S. A.*, 2005, **102**, 4225–4229.
33 A. J. Kim, P. L. Biancaniello and J. C. Crocker, *Langmuir*, 2006, **22**, 1991–2001.
34 P. L. Biancaniello, J. C. Crocker, D. A. Hammer and V. T. Milam, *Langmuir*, 2007, **23**, 2688–2693.
35 V. T. Milam, A. L. Hiddessen, J. C. Crocker, D. J. Graves and D. A. Hammer, *Langmuir*, 2003, **19**, 10317–10323.
36 A. Bunge, A. Kurz, A. K. Windeck, T. Korte, W. Flasche, J. Liebscher, A. Herrmann and D. Huster, *Langmuir*, 2007, **23**, 4455–4464.
37 A. Bunge, M. Loew, P. Pescador, A. Arbuzova, N. Brodersen, J. Kang, L. Dahne, J. Liebscher, A. Herrmann, G. Stengel and D. Huster, *J. Phys. Chem. B*, 2009, **113**, 16425–16434.
38 P. A. Beales and T. K. Vanderlick, *J. Phys. Chem. B*, 2009, **113**, 13678–13686.
39 *IDT oligo analyzer*, http://www.idtdna.com/analyzer/Applications/OligoAnalyzer/.
40 B. E. Lang and F. P. Schwarz, *Biophys. Chem.*, 2007, **131**, 96–104.
41 R. Owczarzy, Y. You, B. G. Moreira, J. A. Manthey, L. Y. Huang, M. A. Behlke and J. A. Walder, *Biochemistry*, 2004, **43**, 3537–3554.
42 J. SantaLucia and D. Hicks, *Annu. Rev. Biophys. Biomol. Struct.*, 2004, **33**, 415–440.
43 P. A. Beales, C. L. Bergstrom, J. T. Groves and T. K. Vanderlick, 2010, submitted.
44 B. Dekruijff and P. R. Cullis, *Biochim. Biophys. Acta*, 1980, **602**, 477–490.
45 J. M. Seddon, R. D. Kaye and D. Marsh, *Biochim. Biophys. Acta*, 1983, **734**, 347–352.
46 S. M. Bezrukov, *Curr. Opin. Colloid Interface Sci.*, 2000, **5**, 237–243.
47 M. Delcea, A. Yashchenok, K. Videnova, O. Kreft, H. Mohwald and A. G. Skirtach, *Macromol. Biosci.*, 2010, **10**, 465–474.
48 S. Mitragotri and J. Lahann, *Nat. Mater.*, 2009, **8**, 15–23.

49 E. Andrianantoandro, S. Basu, D. K. Karig and and R. Weiss, *Mol. Syst. Biol.*, 2006, **2**, 2006.0028.
50 A. C. Forster and G. M. Church, *Genome Res.*, 2007, **17**, 1–6.
51 P. E. M. Purnick and R. Weiss, *Nat. Rev. Mol. Cell Biol.*, 2009, **10**, 410–422.
52 C. Chiarabelli, P. Stano and P. L. Luisi, *Curr. Opin. Biotechnol.*, 2009, **20**, 492–497.
53 G. Murtas, *Mol. BioSyst.*, 2009, **5**, 1292–1297.
54 P. Schwille and S. Diez, *Crit. Rev. Biochem. Mol. Biol.*, 2009, **44**, 223–242.